Finite-size-scaling ansatz for the helicity modulus of the triangular-lattice three-spin interaction model

Hiromi Otsuka

Department of Physics, Tokyo Metropolitan University, Tokyo 192-0397, Japan

The Berezinskii-Kosterlitz-Thouless-type continuous phase transition observed in the three-spin interaction model is discussed. The relevant field theory describes the topological defects involved and enables us to perform the renormalization-group analysis. Based on it, we shall propose the finite-size-scaling ansatz for the helicity modulus, which exhibits the exponent $\bar{\nu}=3/5$ for the correlation length in the disordered phase. We perform the Monte Carlo simulations to confirm the ansatz. Also, we argue its relevance to the ground-state phase transition in the quantum spin chain.

I. INTRODUCTION

The universality observed in the phase transitions is one of the most important phenomena to understand the interaction effects. For the two-dimensional (2D) critical systems other than those with intrinsic anisotropy, it is pronouncedly expressed by the conformal symmetry, and the corresponding field theories are characterized by the central charge c [1]. In the case $c<1$, it appears to almost specify the universality class, i.e., the possible set of the critical exponents [2]. However, for larger values of c, there still exist considerable efforts to understand their universalities, which are possibly related to the exotic phase transitions observed in the complicated systems. It is widely known that the frustration effects sometimes bring about the critical ground states as well as the finite-temperature critical points with larger values of $c \geq 1$. Thus, they have been gathering great attention over the years. On another front, the multispin interactions appear to include the same effect: The exactly solved Baxter-Wu model, consisting of the three-Ising-spin product interaction, is the most basic one [3], which belongs to the same universality class as the four-state Potts ferromagnet [4]. The Ising and the four-state Potts criticalities are of $c=1/2$ and 1, respectively. Thus, the multispin interactions can be expected as another source to bring about the larger value of c.

In this paper, we investigate the three-spin interaction model (TSIM) introduced by Alcaraz *et al.* [5]. Suppose that $\langle k,l,m \rangle$ denotes three sites at the corners of each elementary plaquette of the triangular lattice Λ (which consists of three sublattices Λ_a, Λ_b, and Λ_c), then the following reduced Hamiltonian expresses a class of TSIM:

$$\beta H = -\frac{J}{k_B T} \sum_{\langle k,l,m \rangle} \cos(\varphi_k + \varphi_l + \varphi_m). \quad (1)$$

The angle variables $\varphi_k \in [0,2\pi)$ are located on sites, and the model parameter, the temperature T, will be measured in units of J/k_B. In the previous paper [6], we discussed an effective field theory for a related model (i.e., its clock version) and predicted the one with $c=2$, which was followed by the numerical confirmation based on the transfer-matrix calculations. Here, we perform the renormalization-group (RG) analysis to predict the Berezinskii-Kosterlitz-Thouless (BKT)-type [7,8] phase transition between the critical and the disordered phases. In particular, we shall propose the finite-size-scaling (FSS) ansatz for the helicity modulus representing the stiffness of the corresponding interface model [9,10]. The discussion goes on in a parallel way with the $c=1$ BKT transition case [11], and the ansatz includes the exponent $\bar{\nu}$ for the correlation length. However, since the topological defects involved (for its definition, see below) are not described by the scalars (vortexes), but by the vectors [5] like the Burgers vectors for the dislocations in the 2D melting [12,13], some modifications occur in the RG analysis, and then bring about $\bar{\nu}=3/5$. The FSS ansatz permits us to check it directly by the numerical method, and then provides solid evidence to support the theoretical prediction on the instability in the $c=2$ criticality.

II. THEORY

The fact that the system is invariant under the global spin rotations, $\varphi_k \rightarrow \varphi_k + \sum_{\rho=a,b,c} \sum_{l \in \Lambda_\rho} \psi_\rho \delta_{k,l}$, with the condition $\psi_a + \psi_b + \psi_c = 0$ (mod 2π), is important. Although this U(1) $\times$ U(1) symmetry defined by two independent phases, say $\psi_{a,b}$, is not broken and gives the low-temperature critical phase, it specifies the possible type of perturbations to bring about the high-temperature disordered phase. According to Ref. [6], the following vector sine-Gordon Lagrangian density is relevant to the effective description:

$$\mathcal{L} = \frac{K}{4\pi} \|\partial_i \mathbf{\Phi}(\mathbf{x})\|^2 + \frac{y_1}{2\pi a^2} \sum_{\|\mathbf{N}\|=1} :e^{i\mathbf{N}\cdot\mathbf{\Theta}(\mathbf{x})}:. \quad (2)$$

The symbol : : denotes the normal ordering and means the subtraction of contractions of fields between them; $\| \|$ indicates the norm of the vector, and a gives a short-distance cutoff. The parameter y_1 stands for the effective fugacity to control the appearance of topological defects [6]. $\mathbf{\Phi}(\mathbf{x})$ is the two component vector field attached at the position $\mathbf{x}$ in the basal 2D space, so the first term represents the interface model, where K gives its stiffness. The above symmetry is realized as the periodicity of the field, i.e., $\mathbf{\Phi} \equiv \mathbf{\Phi} + 2\pi\mathbf{e}_\alpha$ ($\alpha=1,2$), where $\mathbf{e}_{1,2}$ are the normalized fundamental vectors of the so-called repeat lattice $\mathcal{R}$ [14] isomorphic to the triangular lattice [6]. Then, the interface can acquire the discontinuity of the amount $2\pi\mathbf{N}$ with $\mathbf{N} \in \mathcal{R}$. The second term

consists of the vertex operators where $iK\partial_i\mathbf{\Phi}=\epsilon_{ij}\partial_j\mathbf{\Theta}$, and creates the shortest discontinuities among possible ones (i.e., the length $\|\mathbf{N}\|=1$). From the RG viewpoint, these topological defects controlled by y_1 are enough to be kept in the theory because these are the most relevant ones (see below).

The reason why we have started with the Lagrangian density instead of the vector Coulomb gas (CG) representation [5] is that, for the RG analysis we shall employ the conformal field theory (CFT) technology, which requires the scaling dimensions of local density operators and the operator-product-expansion (OPE) coefficients among them. While details of their derivations on the Gaussian fixed point (i.e., the first term) will be given in our future report [15], here we shall summarize the relevant results to the present case. Since the low-temperature critical phase corresponds to the Gaussian fixed line parametrized by K, the so-called $\mathcal{M}$ operator [17],

$$\mathcal{M}(\mathbf{x}) \equiv \frac{Ka^2}{\sqrt{8}}\|\partial_i\mathbf{\Phi}(\mathbf{x})\|^2, \qquad (3)$$

which shifts the system along the line, is the most important one. Since $\langle\mathcal{M}(\mathbf{x})\mathcal{M}(\mathbf{0})\rangle_0=(a/r)^4$ independently of K (r is the distance between $\mathbf{0}$ and $\mathbf{x}$), it is truly marginal. On the other hand, the normalized form of the second term in Eq. (2) is given as

$$\mathcal{W}(\mathbf{x}) \equiv \frac{1}{\sqrt{6}}\sum_{\|\mathbf{N}\|=1} :e^{i\mathbf{N}\cdot\mathbf{\Theta}(\mathbf{x})}:, \qquad (4)$$

whose dimension is $x_{\mathcal{W}}\equiv K\|\mathbf{N}\|^2/2=K/2$. Thus, $\mathcal{W}$ becomes marginal at $K=K^*$ ($\equiv4$) and brings about the transition to the disordered phase for $K<K^*$. For later RG argument, the expansion of the operator product $\mathcal{W}(\mathbf{x})\mathcal{W}(\mathbf{0})$ is crucial. While there are 36 terms in the double summations with respect to the vector charges (say $\mathbf{N}$ and $\mathbf{N}'$), the following two cases are enough to be taken into account: (i) $\mathbf{N}+\mathbf{N}'=\mathbf{0}$ and (ii) $\|\mathbf{N}+\mathbf{N}'\|=1$ (the other terms are irrelevant here). After some calculus using the complex coordinate and employing the chiral decomposed form of fields as usual, we find that the cases (i) and (ii) mainly give $\mathcal{M}$ and $\mathcal{W}$, respectively. Then, the expression of the OPE becomes as follows [15,16]:

$$\mathcal{W}(\mathbf{x})\mathcal{W}(\mathbf{0}) \simeq \frac{x_{\mathcal{W}}}{\sqrt{2}}\left(\frac{a}{r}\right)^{2x_{\mathcal{W}}-2}\mathcal{M}(\mathbf{0}) + \frac{2}{\sqrt{6}}\left(\frac{a}{r}\right)^{x_{\mathcal{W}}}\mathcal{W}(\mathbf{0}) + \cdots, \qquad (5)$$

where "$\cdots$" includes the unit operator and the stress tensor as well as less singular terms. Consequently, we can obtain the OPE coefficients $C_{\mathcal{W}\mathcal{W}\mathcal{M}}=x_{\mathcal{W}}/\sqrt{2}$ and $C_{\mathcal{W}\mathcal{W}\mathcal{W}}=2/\sqrt{6}$. The significance of this result is as follows: Due to the triangular lattice structure of $\mathcal{R}$, three vector charges at the angle of $120°$ to each other (e.g., $\mathbf{e}_1$, $-\mathbf{e}_1+\mathbf{e}_2$, and $-\mathbf{e}_2$) satisfy the vector charge neutrality condition, and then provide the nonzero value of $C_{\mathcal{W}\mathcal{W}\mathcal{W}}$. This brings about the difference from the BKT transition (see below).

Now, the RG equations are derived as follows. Suppose that the critical fixed point is perturbed by the marginal scalar operators $\mathcal{O}_\mu(\mathbf{x})$ (normalized) as $\mathcal{L}=\mathcal{L}_0^*+\Sigma_\mu\lambda_\mu\mathcal{O}_\mu/2\pi a^2$, then, the RG equations for the change of the cutoff $a\rightarrow(1$
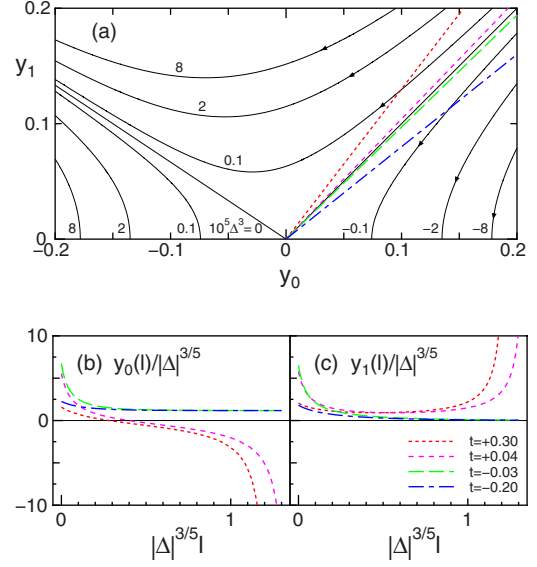

FIG. 1. (Color online) (a) The contour plot of Δ^3 indicating the RG flow. Numerical values near the contour lines in black denote $10^5\times\Delta^3$. The straight lines in color show $y_1(0)=(1+t)y_0(0)$ for some values of t: 0.30 (red dotted line), 0.04 (pink short-dashed line), -0.03 (green dashed line), and -0.20 (blue dot-dashed line). [(b) and (c)] The scaled couplings $y_{0,1}/|\Delta|^{3/5}$ are given as functions of the scaled variable $|\Delta|^{3/5}l$.

$+dl)a$ are given by $d\lambda_\mu/dl=-(1/2)\Sigma_{\nu,\rho}C^*_{\mu\nu\rho}\lambda_\nu\lambda_\rho$ within the one-loop calculations [18]. For the present case of the couplings y_0 ($\equiv K/K^*-1$) and y_1, the equations become

$$\frac{dy_0(l)}{dl}=-3y_1(l)^2, \qquad \frac{dy_1(l)}{dl}=-2y_0(l)y_1(l)-y_1(l)^2. \quad (6)$$

Whereas these are similar to the BKT RG equations [7,8], the y_1^2 term emerges in the second equation due to the non-vanishing coefficient $C_{\mathcal{W}\mathcal{W}\mathcal{W}}$ (see also [5]). Now, we shall discuss its consequences. Like to the BKT transition case, these equations possess a conserved quantity, but unlike to the case, it is given as a homogeneous expression of degree five in y_0 and y_1 as

$$\Delta^3 \equiv (y_1-y_0)^3\left(y_1+\frac{2}{3}y_0\right)^2 \qquad (\Delta\in\mathbb{R}). \qquad (7)$$

Figure 1(a) gives the contour plot with arrows to show the trajectories of the RG flows. Then, we see that the line $y_1=y_0$ is the separatrix between the critical and the disordered phases, so the small parameter for the phase transition can be introduced as $y_1(0)=(1+t)y_0(0)$, with $|t|\ll1$. Now, with the aid of the conservation law, we can analyze the RG flows and obtain the following form:

$$y_{0,1}(l)=|\Delta|^{3/5}g_{0,1}^\pm(|\Delta|^{3/5}l+\tau_t), \qquad (8)$$

where the superscript "$\pm$" indicates the sign of Δ and τ_t is a certain function of t given by the initial values of the couplings [19,20]. This form exhibits a kind of self-similarity that the trajectories with the initial conditions having the same values of t [e.g., all points on the red dotted line in Fig. 1(a)] fall into a single curve independently of Δ [the red

dotted line (a numerical integration) in Fig. 1(b) or 1(c)], and that the t dependence can be absorbed by changing the origin of the scaled variable according to τ_t (the red dotted line overlaps with the pink short-dashed line). The explicit forms of $g_{0,1}^{\mp}$ are complicated while those in the BKT transition are the trigonometric or the hyperbolic functions [19,20]. Nevertheless, we can extract some properties because they share the basic feature with the BKT transition case. On the separatrix $t=0$, the solution is simply given by $y_{0,1}(l)=y(l)\equiv 1/3(l+l_{T_c})$, with $l_{T_c}\equiv 1/3y(0)$. Around it, we find $y_{0,1}(l)\simeq y(l)-[(1\pm 2)/4](3/5)^{2/3}\Delta/y^{2/3}(l)$ when $|t|^{3/5}(l/l_{T_c})\ll 1$ is satisfied (the upper sign refers to the former). Note that these expressions exhibit the nonsingularities of $y_{0,1}(l)$ at $\Delta=0$ and also that they can be regarded as the expansions of the following scaling forms:

$$y_{0,1}(l) \simeq (l+l_{T_c})^{-1}\Psi_{0,1}[\Delta(l+l_{T_c})^{5/3}] \qquad (9)$$

with $\Psi_{0,1}(X)\simeq 1/3+O(X)$. To cast these into the forms compatible with Eq. (8), we should further replace l_{T_c} by a temperature dependent parameter $l_T\equiv\tau_t/|\Delta|^{3/5}$. However, since l_T means the logarithmic scale to obtain the initial values $y_{0,1}(0)$ from $y_{0,1}\simeq\infty$ lying almost on the separatrix, it is a smooth function and can be represented by its value at the transition point l_{T_c}, near T_c.

Now, we shall estimate the correlation length from Eqs. (8) and (9). When we write the characteristic logarithmic scale as l_F satisfying the condition $y_0(l_F)=-\infty$, then $\xi(T)\propto\exp(l_F)$. Figure 1(b) exhibits $g_0^+(\tau\simeq 1.4)=-\infty$, and Δ is proportional to $T-T_c$ near T_c. Thus, we obtain $\xi(T)\propto\exp[\text{const}/(T-T_c)^{\bar\nu}]$, with the exponent $\bar\nu=3/5$. Unlike to the BKT transition case $\bar\nu=1/2$ [7,8], our theory predicts the above exponent, which is attributed to the nature of the topological defects characterized by the vector charges, and more precisely to the nonvanishing OPE coefficient $C_{\mathcal{WWW}}$. However, our result also disagrees with the previous one based on the vector CG representation [5]. Therefore, the numerical evidence to support our theory is desired.

In the remainder of the paper, we shall provide the evidence with the use of the Monte Carlo (MC) method. For this purpose, here we explain the FSS property of the helicity modulus to focus on below. The helicity modulus is defined as the response of the free energy against the long-wavelength (λ) twist of the local order field, which is proportional to the square of the wave number $q\equiv 2\pi/\lambda$, i.e., $\Upsilon(T)\equiv\lim_{q\to 0}\partial^2 f(T,q)/\partial q^2$ [9,10]. For the present model with the $U(1)\times U(1)$ symmetry, the twist can be imposed by, for instance, $\forall\ l\in\Lambda_b$; $\varphi_l\to\varphi_l+\mathbf{q}\cdot\mathbf{x}_l$ and $\forall\ m\in\Lambda_c$; $\varphi_m\to\varphi_m-\mathbf{q}\cdot\mathbf{x}_m$, where $\mathbf{x}_l$ ($\mathbf{x}_m$) is the position vector of the lth (mth) site and $\hat{\mathbf{q}}\equiv\mathbf{q}/q$ is a unit vector in the x direction of the basal 2D space. Then, one finds the following expression:

$$\Omega\Upsilon(T)=\left\langle-\frac{1}{2}H-\frac{1}{T}\left(\sum_{\langle klm\rangle}\sin\varphi_t\ \hat{\mathbf{q}}\cdot\mathbf{x}_{lm}\right)^2\right\rangle, \qquad (10)$$

where $\varphi_t\equiv\varphi_k+\varphi_l+\varphi_m$, $\mathbf{x}_{lm}\equiv\mathbf{x}_l-\mathbf{x}_m$, and Ω is the 2D volume of the system. While this is useful for numerical estimations of Υ, its theoretical expression is also obtained as follows. According to Ref. [6], the above twist corresponds to the following shift in the vector field: $\Phi(\mathbf{x})\to\Phi(\mathbf{x})+\mathbf{q}\cdot\mathbf{x}(-\mathbf{e}_1$

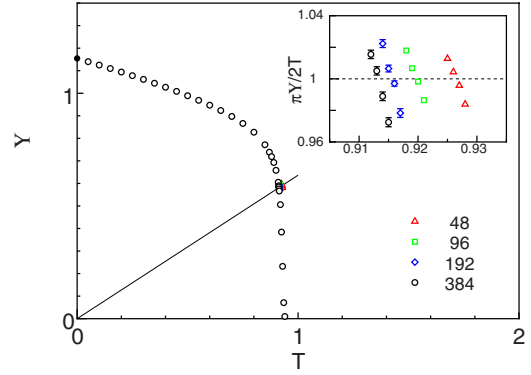FIG. 2. (Color online) Temperature dependence of the helicity modulus. The solid line exhibits $2T/\pi$, and the filled circle is $\Upsilon(0)=\zeta$. The inset gives the magnified view near the transition temperature, where $\pi\Upsilon/2T$ is plotted against T.

$+\mathbf{e}_2$), which then brings about the increase of the Gaussian part in the free energy density $(TK/2\pi)(q^2/2)$. For $T\le T_c$, we can renormalize the effects of the topological defects, so that the helicity modulus in the full theory is given by $\Upsilon(T)=TK(l=\infty)/2\pi$. As usual, the ratio $\pi\Upsilon(T)/2T$ exhibits the universal jump from 1 to 0 at $T=T_c$ in the thermodynamic limit although it is rounded off in the finite-size systems. Relating to this, Harada and Kawashima performed the MC simulations of the 2D quantum XY model, and gave the FSS analysis of the helicity modulus to confirm the BKT theory being valid there [11]. According to their discussion, here we propose the FSS form for the present phase transition: For the finite-size systems with the linear dimension L near T_c, $l+l_{T_c}$ and Δ in Eq. (9) are replaced by the logarithmic scale $\ln(L/L_0)$ (L_0 could depend on the temperature) and $T-T_c$, respectively. Then, we obtain

$$\frac{\pi\Upsilon(T,L)}{2T}-1=\frac{\Psi_0\{(T-T_c)[\ln(L/L_0)]^{5/3}\}}{\ln(L/L_0)}, \qquad (11)$$

where T_c and L_0 are the parameters to be determined based on the FSS ansatz.

III. NUMERICAL CALCULATIONS

Here, we shall provide the MC data of the helicity modulus and its FSS analysis (the details of our simulations will be given elsewhere). Using the standard Metropolis algorithm, the systems of sizes up to $L=384$ were treated. The 10^7 MC steps (MCS) were used for samplings after the 10^6 MCS for equilibration. At each temperature, we performed the independent runs up to 64 so as to attain reliable statistics of data. In units of the squared lattice constant $a^2=1$, the volume is given as $\Omega=L^2/\zeta$, where ζ ($=2/\sqrt{3}$) is the geometric factor of Λ. Then, we obtain the helicity modulus given in Fig. 2. As expected, it exhibits the steep decrease and crosses the straight line $2T/\pi$ (see the circles for $L=384$). Since Υ stands for the stiffness of the interface, its reduction to 0 indicates a kind of melting. The inset gives the magnified view near the transition temperature, where $\pi\Upsilon/2T$ is plotted against T. Thus, the crossings with the dotted line provide
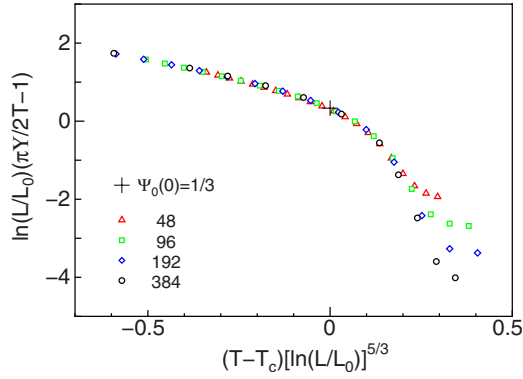
FIG. 3. (Color online) The FSS plot of the helicity modulus. $T_c = 0.907$ and $L_0 = 6.5$ are employed according to the best by-eye scaling. The cross + shows the theoretical prediction on the scaling function $\Psi_0(0) = 1/3$ (see the text).

the finite-size estimates of T_c, $T_c(L)$. In Fig. 3, we show the FSS plot of Υ. According to Eq. (11), the parameters T_c and L_0 were searched until the best collapsing of the scaled data is achieved. Actually, we performed it by eye and obtained the values $T_c \simeq 0.907$ and $L_0 \simeq 6.5$. Then, the figure exhibits that the scaling region is narrow in the upper side of T_c: For $L \geq 192$, it continues up to about 0.25 in the abscissa (see the diamonds and circles). Although this is due to the limitation on the size treated, and further to the property of Υ showing the jump in the thermodynamic limit, we can check the reliability of our FSS analysis as follows. As in the case of the BKT transition, we can extrapolate the finite-size estimates as $T_c(L) = T_c(\infty) + c_1/(\ln L + c_2)^{5/3}$, where $T_c(\infty)$ and $c_{1,2}$ are the least-squares-fitting parameters. Then, we obtain $T_c(\infty) \simeq 0.905$, which agrees well with the FSS result. Further, as argued, the scaling function is theoretically expected to satisfy $\Psi_0(0) = 1/3$. We denote this condition by the cross in Fig. 3 and then we find the good coincidence with the FSS analysis. With respect to the possibility of $\bar{\nu} \neq 3/5$, we tried

the FSS analysis with its value, for instance, 2/5, but the goodness of the scaling in Fig. 3 could not be reproduced within our search. Consequently, these numerical data and the consistencies among them strongly support our field theoretical description on the BKT-type phase transition observed in TSIM [21].

IV. DISCUSSIONS AND SUMMARY

We shall mention the relevance of our theory to other systems. The bilinear-biquadratic spin-1 chain is exactly solvable in some cases. The Uimin-Lai-Sutherland (ULS) point is one of them, on which the low-energy excitations are described by the level-1 SU(3) Wess-Zumino-Witten model ($c = 2$), and by which the massless quadrupole and the massive Haldane phases are separated [22]. This ground-state phase transition was clarified to be BKT-type, and in terms of the small parameter to control the distance from the ULS point, the correlation length is given in the identical form as the present one (i.e., $\bar{\nu} = 3/5$) [23]. Therefore, we think that the phase transition discussed here may share the same fixed-point properties with it; we shall discuss this issue more closely in our future study [15]. To summarize, based on the vector sine-Gordon field theory, we have discussed the continuous phase transition observed in TSIM; the FSS ansatz for the helicity modulus was proposed based on the RG analysis. Our theoretical predictions were confirmed by the use of the MC simulations.

[1] A. A. Belavin, A. M. Polyakov, and A. B. Zamolodchikov, Nucl. Phys. **241**, 333 (1984).
[2] D. Friedan, Z. Qiu, and S. Shenker, Phys. Rev. Lett. **52**, 1575 (1984).
[3] R. J. Baxter and F. Y. Wu, Phys. Rev. Lett. **31**, 1294 (1973).
[4] F. C. Alcaraz and J. C. Xavier, J. Phys. A **32**, 2041 (1999).
[5] F. C. Alcaraz, J. L. Cardy, and S. Ostlund, J. Phys. A **16**, 159 (1983), and the references therein.
[6] H. Otsuka, J. Phys. Soc. Jpn. **76**, 073002 (2007).
[7] V. L. Berezinskii, Sov. Phys. JETP **34**, 610 (1972).
[8] J. M. Kosterlitz and J. D. Thouless, J. Phys. C **6**, 1181 (1973); J. M. Kosterlitz, *ibid.* **7**, 1046 (1974).
[9] M. E. Fisher, M. N. Barber, and D. Jasnow, Phys. Rev. A **8**, 1111 (1973).
[10] D. R. Nelson and J. M. Kosterlitz, Phys. Rev. Lett. **39**, 1201 (1977); T. Ohta and D. Jasnow, Phys. Rev. B **20**, 139 (1979).
[11] K. Harada and N. Kawashima, Phys. Rev. B **55**, R11949 (1997); J. Phys. Soc. Jpn. **67**, 2768 (1998).
[12] B. I. Halperin and D. R. Nelson, Phys. Rev. Lett. **41**, 121 (1978); D. R. Nelson and B. I. Halperin, Phys. Rev. B **19**,

2457 (1979); D. R. Nelson, *ibid.* **18**, 2318 (1978).
[13] A. P. Young, Phys. Rev. B **19**, 1855 (1979).
[14] J. Kondev and C. L. Henley, Phys. Rev. B **52**, 6628 (1995); Nucl. Phys. **464**, 540 (1996).
[15] H. Otsuka and K. Nomura, e-print arXiv:0803.3114.
[16] J. Polchinski, *String Theory* (Cambridge University Press, England, 1998), Vol. I.
[17] L. P. Kadanoff, Ann. Phys. **120**, 39 (1979); L. P. Kadanoff and A. C. Brown, *ibid.* **121**, 318 (1979).
[18] A. M. Polyakov, Sov. Phys. JETP **36**, 12 (1973).
[19] For the BKT transition, see A. P. Young and T. Bohr, J. Phys. C **14**, 2713 (1981).
[20] P. Minnhagen, Rev. Mod. Phys. **59**, 1001 (1987).
[21] In Ref. [6], the explanation that $\bar{\nu}$ takes 2/5 was given. But, this should be corrected as $\bar{\nu} = 3/5$.
[22] G. V. Uimin, JETP Lett. **12**, 225 (1970); C. K. Lai, J. Math. Phys. **15**, 1675 (1974); B. Sutherland, Phys. Rev. B **12**, 3795 (1975).
[23] C. Itoi and M. Kato, Phys. Rev. B **55**, 8295 (1997).